Virtual Planar Motion Mechanism Tests of the Autonomous Underwater Vehicle Autosub

A. Phillips, M. Furlong, S.R. Turnock

Abstract— Hydrodynamic derivatives are used to model the manoeuvring performance of proposed and existing hull forms.
A simple robust method, using unsteady RANS simulations is presented to numerically replicate the experimental PMM tests performed on a scale model of the Autonomous Underwater Vehicle (AUV) Autosub. The method uses a body fitted inner domain to capture the unsteady flow. This body fitted mesh moves relative to a fixed outer domain via stretching/compressing cells at the interface. Detailed results for pure sway motion are presented and show good agreement for a relatively low computational cost. It is estimated that at the initial design stage a full set of manoeuvring derivatives could be found for an axis-symmetric AUV or submarine in under two days of simulation time using a desktop pc.

***Index Terms*—Autonomous Underwater Vehicle, Computational Fluid Dynamics, Planar Motion Mechanism Tests, Submerged Body**

Fig. 1. The AUV Autosub Designed And Developed At The National Oceanography Centre, Southampton.

I. Introduction

The manoeuvring of surface ships and submarines is a complex non linear problem with significant coupling between the six degrees of freedom. It is standard practise to decouple the 6 DOF into horizontal and vertical motion, and simplify the problem to a set of linear equations. Using hydrodynamic derivative notation, $\frac{\partial Y}{\partial v} = Y_v$, the linearised equations of motion for a vessel in the horizontal plane are [1]: -

$$-X_u(u-V)+(m-X_{\dot{u}})\dot{u}=0$$
$$-Y_v v+(m-Y_{\dot{v}})\dot{v}-(Y_r-mu_1)r-(Y_{\dot{r}}-mx_g)\dot{r}-Y_\delta\delta=0$$
$$-N_v v-(N_{\dot{v}}-mx_g)\dot{v}-(N_r-mx_g u_1)r+(I_z-N_{\dot{r}})\dot{r}-N_\delta\delta=0$$

The surge and sway velocities u and v are the velocity components of the origin placed at amidships, where V is the initial velocity of the vessel. The yaw rate r is the angular velocity about the vertical axis. X represents the surge force, Y the sway force and N the yaw moment. The Rudder angle is represented by δ.

A, Phillips and S. R. Turnock are with the School of Engineering Sciences, University of Southampton, Southampton SO17 1BJ UK.
M. Furlong is with the National Oceanography Centre, Southampton, UK.

Traditionally the hydrodynamic derivatives for Autonomous Underwater Vehicles (AUV) are derived from a combination of towing tank experiments, [2][3], such as: yawed resistance tests, rotating arm experiments and Planar Motion Mechanism (PMM) tests or through the use of empirical formulas [4].

An alternative method of deriving hydrodynamic derivatives for and AUV or other deeply submerged body is to use Reynolds Averaged Navier Stokes (RANS) simulations to replicate experimental PMM tests numerically.

The use of RANS simulations to assess the straight line performance of surface ships and submarines is well established [5], while current research is targeted at understanding steady and unsteady performance of these vehicles.

Simonson et al [6] investigated the flow structures around the KVLCC2 tanker hull form during steady state drift manoeuvres. Bellevre et al [7] used a combination of translational and rotational steady state RANS simulations to derive the velocity based hydrodynamic derivatives for a submarine, the resulting hydrodynamic model showed good agreement with full scale sea trials. The use of steady state simulation precludes the calculation of acceleration based

hydrodynamic derivatives ($Y_{\dot{v}}$, $N_{\dot{v}}$, $Y_{\dot{r}}$ and $N_{\dot{r}}$)

Brogali et al [8] used an in-house CFD code to investigate the blockage effects during PMM tests of the KVLCC2 in three different width model basins. A medium grid with 500,000 elements was used for the unsteady simulations with 127 time steps per period. Motion of the vessel was simulated using an overlapping mesh method with 8 fixed background blocks and 20 fitted blocks moving with the hull. The influence of tank walls on the calculated derivatives was clearly identified.

Hochbaum [9] simulated PMM tests of the NSTL ferry on a course hexahedral grid (206,000 elements) ignoring the free surface. Time steps equal to 1/5000 of the motion period with 8 inner iterations at each time step were calculated resulting in run times of approximately 48 hours. The resulting hydrodynamic derivatives show good agreement with experimental forces with the relative error being less than 22%. The set of experimental and CFD hydrodynamic derivatives were used in two hydrodynamic models and the vessels response to zigzag and spiral manoeuvres assessed. The difference between the experimental and computational model to $10^o/10^o$ zigzag manoeuvres was small, the inaccuracies in the model became pronounced for a $20^o/20^o$ zigzag manoeuvre.

AUV's provide an important tool for collecting detailed scientific information from the ocean depths. The Autosub family of AUVs has been exploring the oceans since 1996. They have been developed by a team of engineers and oceanographers at the National Oceanography Centre, Southampton. Autosub has been employed in scientific research projects ranging from mapping manganese distributions in a sea loch to ground breaking under ice exploration in the Arctic and Antarctic [10][11]. The principle dimensions of Autosub are listed below:

- Length 7 m
- Diameter 0. 9 m
- Speed Range 1.0 - 2 m/s
- Operating Reynolds Number (R_N) 5.9×10^6 - 11.8×10^6

Autosub is controlled by four movable control surfaces mounted at the rear of the vessel in a cruciform arrangement as shown in Fig. 1. Two coupled vertical rudders control the yaw of the vessel, while two coupled horizontal stern planes adjust the pitch of the vessel.

Model scale PMM tests were performed on a near $2/3^{rds}$ scale model of the Autosub hull form by Kimber et al. [9] at the HASLAR Manoeuvring Basin, Gosport (270 m × 12.2 m × 5.5 m deep), and No. 2 Tank (270m × 12.2m × 5.5m deep).

The aim of the program of work underway at the University of Southampton (UoS) is to develop specific AUV hull concept design techniques that are robust and reliable. To this end steady and unsteady CFD analysis methods are being investigated which combine automated meshing and parametric hull shape definitions. This is in order to reduce overheads when evaluating the resistance and manoeuvring of a concept AUV hull. Experimental PMM tests require specialist facilities equipment and a physical model of the geometry not usual available at the initial design stage. Thus the objectives of this study are to: (1) demonstrate the methodology for virtual PMM tests for submerged bodies; (2) benchmark the methodology against existing experimental results; (3) establish the time scales for deriving a full set of hydrodynamic derivatives for a concept AUV.

II. Planar Motion Mechanism Tests

Planar Motion Mechanisms (PMM) consist of two oscillators mounted on a towing tank carriage, one at the bow and one at the stern of the vessel, each imparts a transverse motion on the vehicle as it travels down the tank at a constant velocity. The phase ε between the bow and stern oscillator can be adjusted to produce pure sway, pure yaw or a combination of sway and yaw motion.

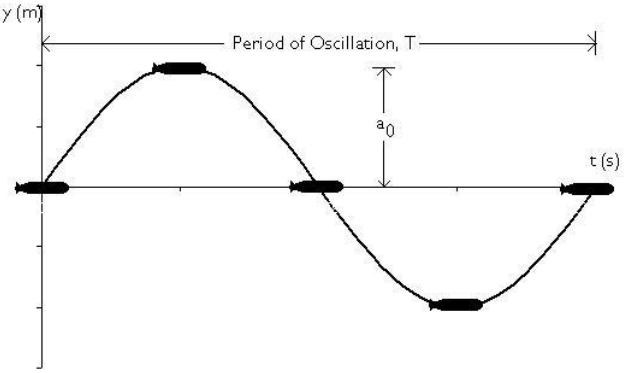

Fig 2. Orientation Of Model Throughout Pure Sway PMM Test.

This paper will discuss pure sway motion (y) which occurs when ε=0, see Fig 2. The variation in sway displacement, velocity and acceleration are given by the following equations.

$$y_0 = y = a_0 \sin \omega t$$

$$\frac{dy}{dt} = v = -a_0 \omega \cos \omega t$$

$$\frac{d^2 y}{dt^2} = \dot{v} = -a_0 \omega^2 \sin \omega t$$

The forces and moments acting on the vessel are monitored in real time as the vessel is oscillated. The velocity based derivatives represent the viscous forces associated with the velocity of the vessel. Y_v and N_v are measured when the velocity is maximum, and the acceleration is zero. The acceleration based derivatives are associated with the added mass of the vehicle $Y_{\dot{v}}$ and $N_{\dot{v}}$ are measured at the same time as the maximum displacement.

III. Methodology

The fluid flow around Autosub has been modelled using the commercial finite volume code ANSYS CFX 11 (CFX) [12]. The motion of the fluid is modeled using the incompressible, isothermal Reynolds Averaged Navier Stokes (RANS) equations in order to determine the cartesian flow field ($u_i = u, v, w$) and pressure (p) of the water around Autosub.

$$\frac{\partial \overline{U_i}}{\partial x_i} = 0$$

$$\frac{\partial \overline{U_i}}{\partial t} + \frac{\partial \overline{U_i U_j}}{\partial x_j} = -\frac{1}{\rho}\frac{\partial P}{\partial x_i} + \frac{\partial}{\partial x_j}\left\{\nu\left(\frac{\partial \overline{U_i}}{\partial x_j} + \frac{\partial \overline{U_j}}{\partial x_i}\right)\right\} - \frac{\partial \overline{u_i' u_j'}}{\partial x_j} + f_i$$

A. Mesh Definition

The Autosub geometry and mesh are generated using Tool Command Language (TCL) script files within ANSYS ICEM CFD. This allows detailed control of the mesh parameters and element quality.

The relatively simple geometry of Autosub lends itself to creating a multi-block structured hexahedral mesh to define the fluid immediately surrounding the AUV, a H grid topology is used in the far field with an O grid topology wrapped around the hull to provide control over boundary layer elements. A first layer thickness of 1mm has been used. This corresponds to $20<y^+<200$, with 10 elements maintained within the boundary layer.

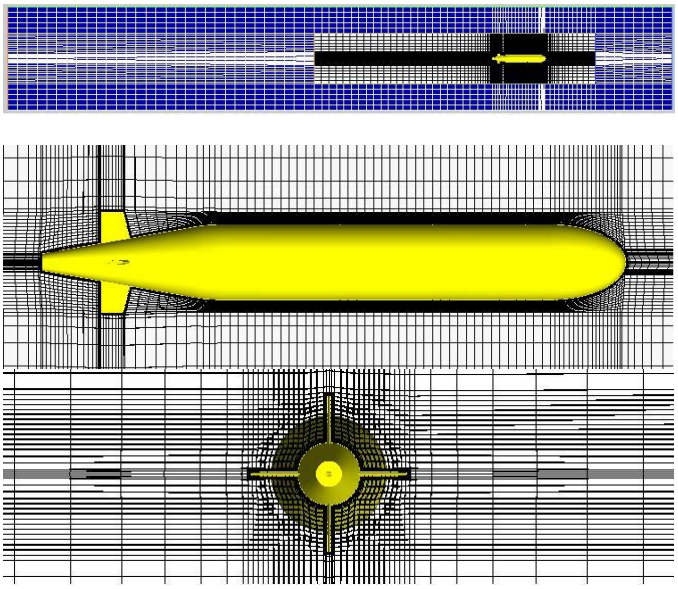

Fig 3. Inner And Outer Domain Meshes (*Top*), Detailed Mesh About Autosub (*Middle*) And Detailed Mesh In The Transverse Plane Through The Control Surfaces (*Bottom*).

B. Mesh Deformation

To replicate the sway motion produced in the experimental PMM tests the Autosub geometry moves within the domain, deforming the mesh. CFX has an inbuilt "mesh morphing" model which is used to calculate the new node locations at each time step, while maintaining mesh topology. The model calculates the displacement on each node using a spring analogy method.

Although the amplitude of the lateral motion (a_0) is small in relation to the vehicle length (L) $a_0/L=0.00544$ it is large in relation to the trailing edge of the rudders. Consequently if the mesh surrounding the vehicle is allowed to deform the elements at the rudder trailing edges skew and quickly form negative volumes.

Thus in order to replicate the motion of the vessel the fluid domain is split into an inner and outer region. The outer domain remains fixed in space while the inner domain containing the hull moves laterally to replicate the motion induced on a PMM. The mesh in the inner sub domain remains locked in position relative to the lateral motion of the vessel. This prevents deformation of the detailed mesh around the vessel. The mesh in the outer region is coarser and deformed due to the motion of the inner region, see Fig 3 and 4.

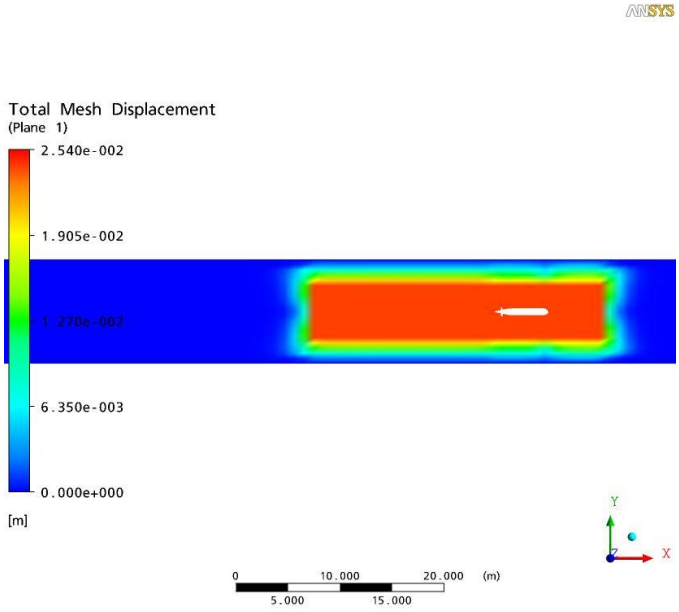

Fig 4. Mesh Displacement Shown At Maximum Sway Displacement With Large Mesh Stretching Only Occurring In The Green Region Well Away From The Induced Flow Structures.

C. Boundary Conditions

The boundary conditions on the domain consist of: -

- The AUV hull is modelled using a no-slip wall condition.
- Dirichlet inlet condition, two body lengths upstream of the AUV where the inlet velocity and turbulence

are prescribed explicitly. The model scale velocity of 2.69m/s is replicated in the CFD analyses this equates to 2m/s full scale. Inlet turbulence is set at 5%.

- Mass flow outlet is positioned nine body lengths downstream.
- On the outer domain four free slip wall conditions 6.5 diameters away from the AUV geometry complete the boundary conditions.

The interface between the inner and outer domain is achieved using six CFX General Grid Interface (GGI) connections. These refer to the class of grid connections where the grid on either side of the two connected surfaces does not match. A major drawback of structured meshes is the inability to rapidly grow elements in the far field. The use of CGI interfaces allows the outer domain to have a significantly coarser mesh density, however it also results in flow properties being artificially averaged by the mesh as fluid flows from the inner domain to the outer domain. To minimise the influence of this effect the domain interfaces have been placed one body lengths upstream, 3 body lengths downstream and at three diameters distance in the radial direction.

D. *Turbulence Models*

By time averaging the Navier Stokes equations to generate the RANS equations, 6 further unknowns have been created, termed the Reynolds stresses. Various turbulence models have been proposed to provide solutions to the Reynolds stresses in terms of known quantities to allow closure of the RANS equations [13]. Different turbulence models have been tailored to different types of turbulent flows. The k−Epsilon model is a commonly used turbulence model for engineering simulations due to its robustness and application to a wide range of flows. However it is known to be poor at locating the onset and extent of separation. An alternative approach, the Shear Stress Transport (SST) model has been found to be better at predicting the separation [14] likely to be found at the aft of the AUV.

E. *Running Simulations*

Initial steady state simulations are performed to provide initial conditions to the transient simulation. Transient CFX simulations are then performed for 1.5 cycles of motion. The first 1/2 cycle allows the system to settle before measurement of the derivatives are made over a complete cycle.

Simulations were run on a high specification desktop pc running 64 bit Windows XP using an AMD Athalon 60 X2 Dual Core Processor 5000+ (2.61GHZ) with 4 GB of RAM. Solutions presented have been calculated using the high resolution advection scheme. The residual mass error was reduced by four orders of magnitude and lift and drag forces on the AUV were monitored to ensure convergence.

IV. Independence Studies

The aim of these studies is to select appropriate mesh and simulation properties for accurate solutions while maintaining the run time for 1.5 period of oscillation to below 24 hours.

A. *Mesh Density*

For steady state simulations of an AUV a mesh density of between 700,000 and 1 million elements has been shown to provide good predictions of the straight line resistance of a deeply submerged AUV. [15]. Since transient simulations are required to solve multiple coefficient loops at each time step, the solution time will be significantly greater than for steady state simulations. Consequently a set of three relatively coarse meshes have been investigated.

TABLE I
Mesh Density

Mesh Density	Elements Inner Domain	Elements Outer Domain	Run Time (1 Oscillation T=1.46s)
Coarse	168508	24732	5 hours 12 min
Medium	438416	93237	10 hours 48 min
Fine	679064	153342	14 hours 14 min

Comparisons of the surge and sway forces and yaw moments predicted for each of the meshes are presented in Fig 5. The predicted drag reduces with increasing mesh density. This is indicative of there being too few elements, in the stagnation region at the bow of the vessel and in the wake region aft of the vehicle, to accurately capture the pressure difference between the bow and stern of the vessel. Sway force predictions are nearly identical for the three meshes while the predicted yaw moment predictions vary slightly.

For all further results the medium mesh has been used to ensure solution times remain close to 24 hours for the longer period oscillations.

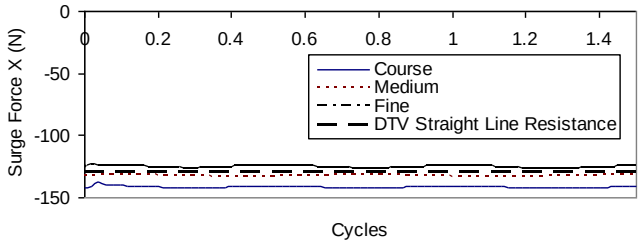

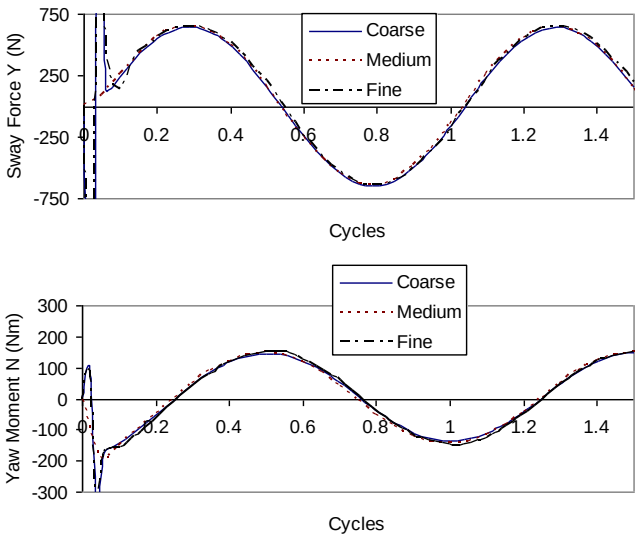

Fig 5. Influence Of Mesh Density On Surge Force (X), Sway Force (Y) And Yaw Moment (N)

B. Time Step

Determining an appropriate time step is necessary to ensure valid results while minimizing the total run time. An initial study was performed considering a period of oscillation of 1.46s. There is significant variation in the number of time steps per oscillation used within the literature. To investigate the effect simulations with 20, 50 and 100 time steps per oscillation were performed.

The results are illustrated in Figure 6. For all three cases significant instabilities are demonstrated during the initial stages of the transient simulation, however the variation of sway force and yaw moment have stabilized after 0.5 oscillations. Time step dependencies are demonstrated in the results, the results for 20 oscillations per cycle while similar in magnitude are out of phase with the forces and moments calculated at 50 and 100 cycles per second. The results for 50 and 100 oscillations per cycle are near to identical demonstrating that for this case 50 oscillations per cycle is sufficient.

50 time steps per oscillation results in a RMS Courant number of 2.82 on the medium mesh. Generally for transient simulations a Courant No. of 1 is desirable, which would require 141 time steps per oscillations. However the oscillations in this simulations are small and thus the unsteadiness may be captured with a reduced number of times steps.

The number of time steps per oscillation is a useful measure for a single period of oscillation, however for the full range of PMM tests four periods are considered 1.46s, 1.75s, 2.19s and 4.66s. Thus for this study the number of time steps required is held constant and determined by the time it takes for the fluid to flow past the AUV, (T_{fp}=L/V) at 59 resulting in a time step of 0.0292s. So the number of time steps per period varies from 50 to 160 for 1.46s and 4.66s respectively

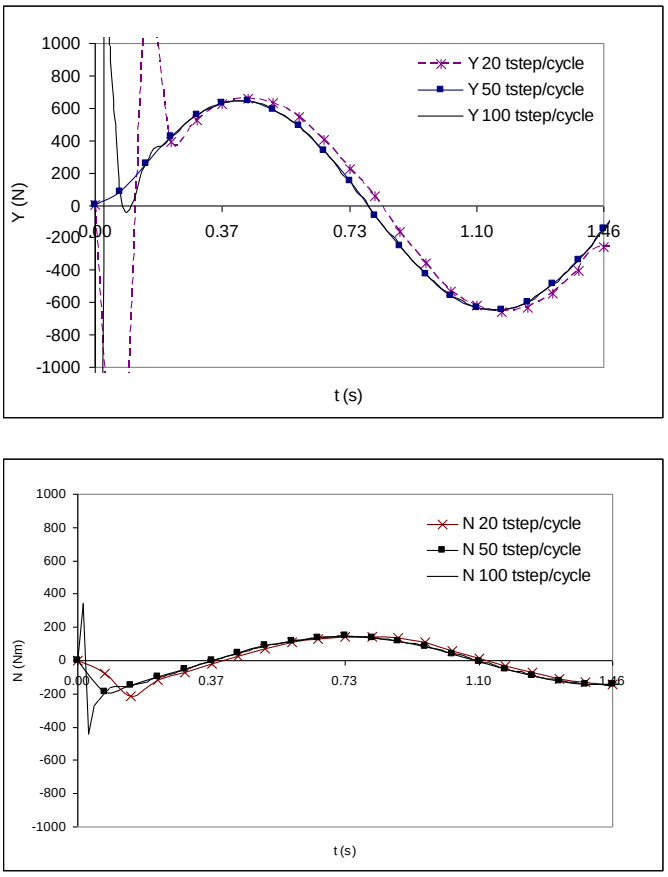

Fig 6. Influence Of The Number Of Time Steps Per Cycle On Sway Force (Y) And Yaw Moment (N)

C. Turbulence Model

Comparison of the force and moments predicted by the SST and K-epsilon turbulence models are presented in Fig 7. Both models provide similar results, however, the SST model stabilizes faster and produces a smoother data set and has consequently been used for the remainder of this work

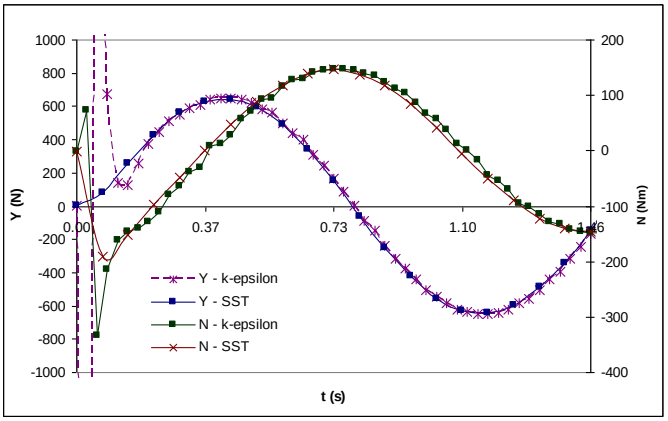

Fig 7. Influence Of The Turbulence Model On Sway Force (Y) And Yaw

Moment (N)

V. RESULTS

As the Autosub is oscillated laterally the flow pattern around the vehicle varies with time. Fig. 8 demonstrates the oscillating wake pattern behind Autosub as the vehicle is oscillated laterally.

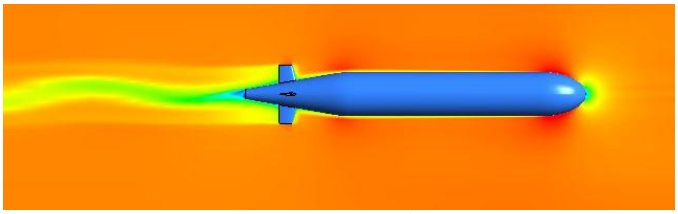

Fig 8. Oscillating Wake Pattern Downstream Of Autosub

Fig 9 illustrates the C_p variation over the hull through one cycle of motion

$$C_p = \frac{P - P_0}{1/2\rho V^2}$$

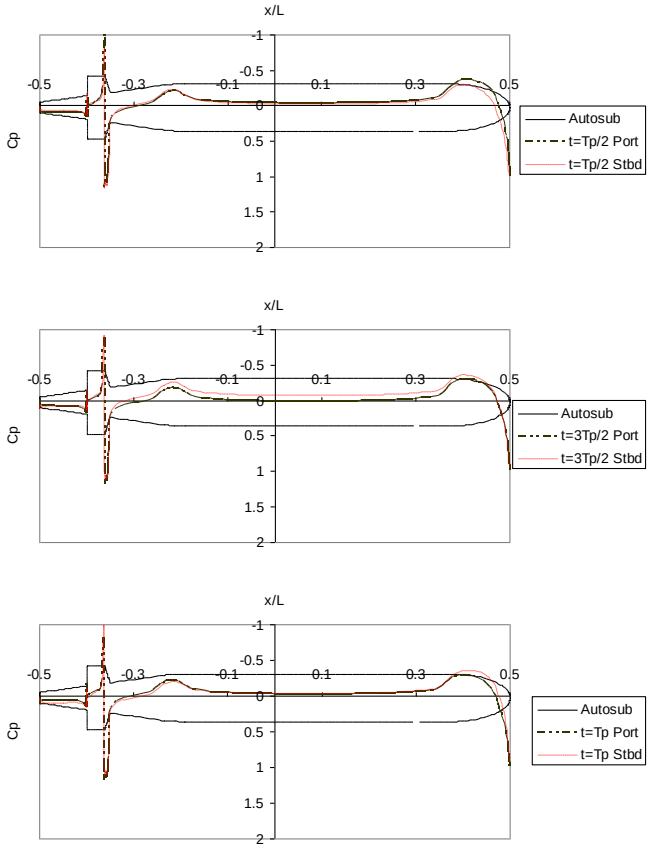

Fig 9. Pressure Variation Over One Period Of Oscillation. Cp Plots Presented Correspond To A Cut Plane Horizontally Through The Centre Of The Vehicle, Thus The Peaks At The Stern Correspond To The Pressure Variation Over The Rudder.

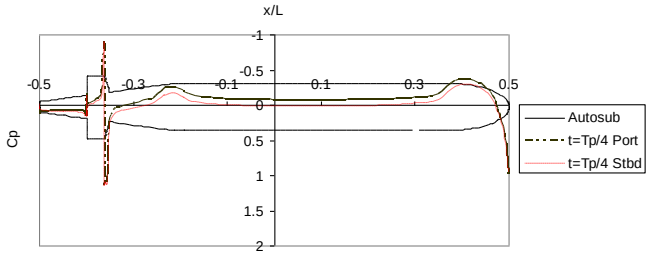

The following plots of forces and moments have been non-dimensionalised using the length of the vehicle (L) the velocity of the vehicle (V) and the density of the fluid (ρ), a prime symbol is used to signify the non dimensional form for example:

$$v' = \frac{v}{V}$$

$$Y' = \frac{y}{1/2\,pL^2V}$$

$$N' = \frac{N}{1/2\,pL^3V}$$

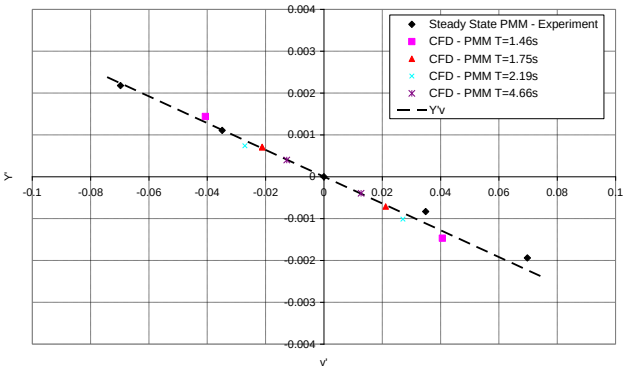

Fig 10. Sway Force versus Sway Velocity

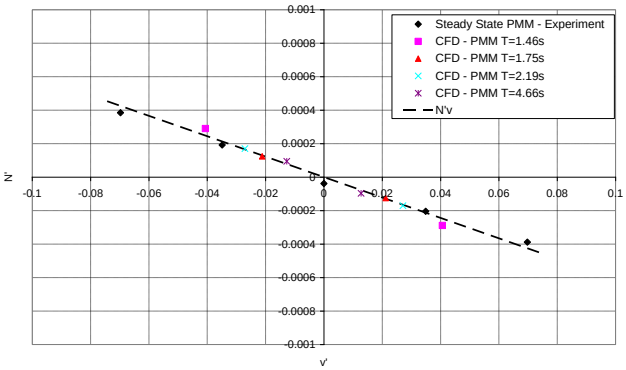

Fig 11. Yaw Moment versus Sway Velocity

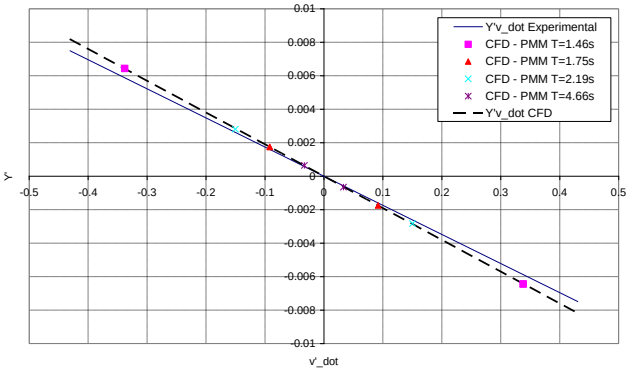

Fig 12. Sway Force versus Sway Acceleration

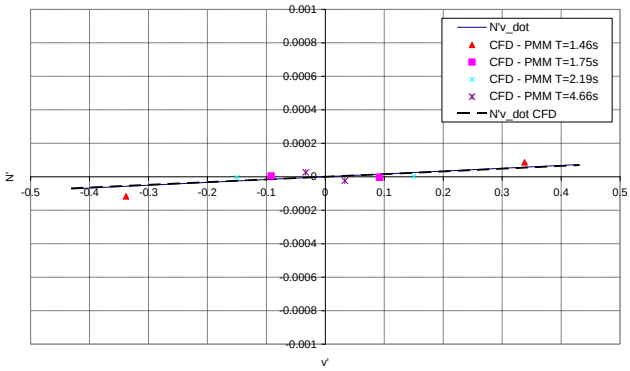

Fig 13. Yaw Moment versus Sway Acceleration

TABLE II
COMPARISON OF DERIVATIVES

Derivative	Experimental x 10^3	CFD x 10^3	E [%]
Y'_v	-29.134	-32.0	8.9
N'_v	-4.539	-6.1	25.6
$Y'_{\dot{v}}$	-17.39	-19.0	8.4
$N'_{\dot{v}}$	0.1691	-0.16	-5.7

VI. DISCUSSION

The numerical simulations are capable of capturing the sway force and yaw moment fluctuations due to pure sway oscillations with relatively coarse mesh densities and time steps. The resulting predictions of the linear velocity and acceleration based derivatives Y'_v, N'_v, $Y'_{\dot{v}}$ and $N'_{\dot{v}}$ show good correlation with the experimental values, see Table II. The assumption of linearity appears to hold for the range of sway velocities and accelerations considered. It should be noted that the error in agreement for the absolute force and moment are in the range 1-8%.

Predominantly steady state manoeuvres such as the turning circle test are dependent on good predictions of the velocity based derivatives, Y'_v, N'_v. Zigzag and other unsteady manoeuvres require knowledge of the acceleration based derivatives in order to understand the influence of added mass on the vessels performance. For a linear model of an AUV operating in the horizontal plane there are 12 hydrodynamic derivatives required. For axi-symmetric vehicles such as Autosub the hydrodynamic derivatives in sway and yaw are equally applicable in heave and pitch providing the vehicle is deeply submerged.

Table III demonstrates the required number of simulations to derive the hydrodynamic derivatives in the horizontal and vertical planes for an axi-symmetric AUV. Assuming the behaviour of each of the derivatives is linear then it is only necessary to perform one of each of the four listed

experiments to derive a preliminary set of derivatives. Assuming a runtime of 15 hours for the unsteady simulations and 30min for the steady state simulation gives a total runtime of 45.5 hours for a preliminary set of derivatives for a single configuration.

TABLE III
REQUIRED SIMULATIONS TO DERIVE A FULL SET OF HYDRODYNAMIC DERIVATIVES FOR AN AXISYMETRIC AUV

Derivative	Pure Surge	Pure Sway PMM	Pure Yaw PMM	Steady State Rudder Angle Tests
X'_u	√			
$X'_{\dot{u}}$	√			
Y'_v (Z'_w)		√		
N'_v ($-M'_w$)		√		
$Y'_{\dot{v}}$ ($Z'_{\dot{w}}$)		√		
$N'_{\dot{v}}$ ($-M'_{\dot{w}}$)		√		
Y'_r ($-Z'_q$)			√	
N'_r (M'_q)			√	
$Y'_{\dot{r}}$ ($-Z'_{\dot{r}}$)			√	
$N'_{\dot{v}}$ ($M'_{\dot{r}}$)			√	
Y'_δ				√
N'_δ				√

At the initial design stage it would ideally be possible to assess a series of hull forms and appendages. Consequently the total simulation time increases rapidly. For instance, to consider three candidate hull forms with three possible appendage sets results in 9 combinations and a simulation time of ~17 days using this method on a single machine. A runtime of 48 hours for a PMM simulation as quoted in the literature [9] would result in a total simulation time of ~54 days.

VII. CONCLUSIONS

A simple robust method for deriving the hydrodynamic derivatives of a submerged body has been presented using virtual PMM tests. Unsteady RANS simulations allow calculation of the acceleration based derivatives which are necessary to model unsteady manoeuvres.

The results have been benchmarked against experimental results showing good replication of experimental values with relatively coarse meshes. This should allow for the initial concept design stage the calculation of a full set of hydrodynamic derivatives for an axis-symmetric AUV or submarine in under two days simulation time using a single desktop pc.

VIII. FURTHER WORK

This work has been performed assuming that the AUV is deeply submerged. The next phase of this work is to expand the discussed methodology to perform virtual PMM tests on a shallowly submerged AUV or a vessel on the free surface.

ACKNOWLEDGEMENTS

Mr Phillips' PhD studentship is jointly financed by the School of Engineering Sciences and the National Oceanography Centre, Southampton.

REFERENCES

[1] J. P. Constock, "Principles of Naval Architecture," SNAME, 1967
[2] N. Kimbler and W. Marshfield, "Design and testing of control surfaces for the Autosub demonstrator test vehicle," DRA Haslar, Tech. Rep., 1993.
[3] J. Guo and F. Chiu. "Manoeuvrability of a Flat-Streamlined Underwater Vehicle," Proceedings of the 2001 IEEE International Conference on Robotics and Automation, 2001
[4] D. E. Perrault, T. Curtis, N. Bose, S. O'Young and C Williams, "C-Scout Manoeuvrability - a Study in Sensitivity," Oceans 01, 2001.
[5] L. Larsson, F. Stern and V, Bertram, "Benchmarking of Computational Fluid Dynamics for Ship Flows: The Gothenburg 2000 Workshop," Journal of Ship Research, volume 47, 1 March 2003
[6] C.D. Simonsen and F. Stern, "Flow Structure Around Manoeuvring Tanker In Deep and Shallow Water," 26th Symposium on Naval Hydrodynamics Rome, Italy, 17-22 September 2006
[7] D. Bellevre, A. Diaz de Tuesta, and P. Perdon, "Submarine Manoeuvrability assessment using Computational Fluid Dynamic Tools". In Proc. 23rd Symposium of Naval Hydrodynamics, Val de Reuil, France, September, 2000.
[8] R. Brogali, R. Muscari, and A. Di Mascio, "Numerical Analysis of Blockage Effects in PMM Tests," In Proc. 26th Symposium on Naval Hydrodynamics Rome, Italy, 17-22 September 2006
[9] A. C. Hochbaum, "Virtual PMM Tests for Manoeuvring Prediction," In Proc. 26th Symposium on Naval Hydrodynamics Rome, Italy, 17-22 September 2006
[10] P. Statham, D. Connelly, C. German, T. Brand, J. Overnell, E. Bulukin, N. Millard, S. McPhail, M. Pebody, J. Perrett, S. M, P. Stevenson, and A. Webb, "Spatially complex distribution of dissolved manganese in a fjord as revealed by high-resolution in situ sensing using the autonomous underwater vehicle Autosub," Environmental Science and Technology, 2005.
[11] P. Wadhams, J. Wilkinson, and S. McPhail, "A new view of the underside of arctic sea ice," Geophysical Research Letters, 2006.
[12] ANSYS CFX, Release 11.0. ANSYS Ltd, 2006..
[13] D. C. Wilcox, Turbulence Modelling for CFD. La Cnada, Calif. : DCW Industries, 1998.
[14] CFX, "Innovative turbulence modelling: SST model in Ansys CFX," ANSYS Ltd, Tech. Rep., 2006.
[15] A. Phillips, M. Furlong and S.R. Turnock, "The Use of Computational Fluid Dynamics to Assess the Hull Resistance of Concept Autonomous Underwater Vehicles," IEEE Oceans 07, Aberdeen, June 2007.